J Mater Sci (2009) 44:2101–2108
DOI 10.1007/s10853-009-3305-2

Processing and thermal stability of a $C_{fiber}/SiC_{filler}/Si–C–N_{matrix}$ composite: effect of oligomer vaporization and the surface oxide layer of SiC filler

Sea-Hoon Lee · Fritz Aldinger

Received: 23 September 2008 / Accepted: 28 January 2009 / Published online: 26 February 2009

Abstract The processing of carbon fiber-reinforced ceramic matrix composites (CMC) made by the precursor impregnation and pyrolysis (PIP) method was improved, and factors which deteriorate the thermal stability of the CMC were investigated. The processing time for cross-linking of a precursor polymer was substantially reduced by the application of a sealed metal container due to the suppression of the vaporization of oligomers. The strength of the as-fabricated CMC was 286 MPa and 77% of the original strength was retained after a heating at 1350 °C for 24 h in Ar. The reduction of the strength after the heating was due to the decomposition of SiO_2 which remained at the surface of the SiC filler particles. The decomposition reaction induced deterioration of carbon fibers and the matrix of the CMC at high temperature.

Introduction

Ceramic matrix composites (CMC) are promising candidates for reliable applications at high temperature [1]. Techniques such as chemical vapor infiltration (CVI), liquid silicon infiltration (LSI), and precursor impregnation and pyrolysis (PIP) have been most frequently reported as fabrication methods of CMC. Composites made by the first route have superior high temperature properties compared to those made by the latter two (LSI and PIP) techniques [2]. LSI and PIP technique benefit from the low production costs [3]. However, a silicon melt formed during the exposure of CMC made by LSI method at high temperatures acts as a source of failure [4, 5]. The PIP technique does not suffer from such problems and therefore has been intensively investigated during the last two decades for the fabrication of CMC [6].

The general procedure of the PIP technique is first, impregnating woven fiber fabrics with a liquid polymer, second, cross-linking the polymer by heating or UV irradiation, and finally pyrolyzing it at elevated temperatures (1000–1400 °C) in a controlled atmosphere.

Important properties of precursor polymers, such as viscosity, vapor pressure, and ceramic yield, depend to a great extent on the degree of cross-linking, and thus can be optimized by proper heat treatments. However, such heat-treatments cause evaporation of low molecular weight oligomers in the precursors, which frequently results in weight loss [7] and flaw formation of the material. In spite of the importance, improvement of the cross-linking process has not been so frequently investigated for the PIP technique [8, 9].

Tanaka et al. [10] reported that although the open porosity of CMC could be decreased to 5% after 10 times of impregnation, the overall relative density was still only 83% since they contained large closed pores between the fiber yarns. In order to reduce the volume of free space which have to be filled by impregnation, filler materials such as SiC have been applied in PIP technique [11]. Researches have been performed concerning the effect of filler materials on the mechanical properties of CMC

S.-H. Lee · F. Aldinger
Max-Planck-Institut für Metallforschung and Institut für Nichtmetallische Anorganische Materialien, Universität Stuttgart, Pulvermetallurgisches Laboratorium,
Heisenbergstrasse 3, Stuttgart 70569, Germany

S.-H. Lee (✉)
Korea Institute of Materials Science (KIMS),
531 Changwondaero, Changwon, Gyeongnam 641831,
Republic of Korea
e-mail: seahoon1@kims.re.kr

[12, 13], but their effects on the high temperature stability of fiber-reinforced CMC have been rarely reported.

In the present investigation, the processing of a CMC composed of carbon fiber fabrics, SiC filler, and Si–C–N precursor-derived ceramic matrix (termed C_{fiber}/SiC_{filler}/$Si–CN_{matrix}$) was improved in terms of cross-linking, and the microstructure, mechanical properties, and high temperature stability of the resultant CMC were analyzed. In addition, the possible deterioration mechanisms of the CMC after a heating at 1350 °C in Ar were discussed.

Experimental procedure

Twelve layers of 2D-woven carbon fiber fabrics (Fiber: T300J-3K-40, Toray. Weaving and coating: M&T Verbundtechnologie GmbH, total thickness ~4 mm) were stacked in a mold, and infiltrated with an aqueous slurry composed of 43 vol.% SiC (A-10, H. C. Starck, d_{50}: 0.51 µm, oxygen content: 0.9 wt%) and 1.5 wt% PEI (polyethylenimine, Aldrich Chem., Mw: 25,000) as a dispersant. The pH of the slurry was adjusted to 6.5 by 1 mol% HCl [14]. A modified infiltration technique was applied for the homogeneous distribution of the filler particles between the woven fabrics by the application of a mold with a deformable wall [14]. The inner space of the mold could expand during slurry infiltration, which enhanced penetration of the viscous slurry into the woven fabric layers. After the infiltration, the molds were placed in an oven first at 80 °C for 24 h for drying the C_{fiber}/SiC_{filler} compact and then at 350 °C for 6 h in vacuum to remove the residual moisture.

For the formation of the matrix, a commercially available liquid Si–C–N precursor (VL 20, KION) was dissolved in de-hydrated tetrahydrofuran (1:1 by volume) in order to decrease its viscosity for impregnation. Currently SiC precursors are commercially available, but they should be kept below −10 °C for the storage [15]. In contrast, Si–C–N based precursors can be stored at room temperature up to 5 years, thus are friendlier for commercialization [16]. After the impregnation, the solvent was removed by evacuating the mold at 40 °C for 6 h. The mold was then capped and heated for cross-linking the precursor in two devices providing different conditions (Fig. 1). The equipment shown in Fig. 1a is a conventionally used glass tube equipped with a gas bubbler for an easy release of gaseous species formed during cross-linking. In order to reduce the vaporization of the precursor during cross-linking, a sealed stainless steel container as shown in Fig. 1b was developed. The inner free volume of the container was minimized and it could sustain increased pressure caused by the evaporation. A dish containing a small amount of excess precursor was placed in the container so that the equilibrium vapor pressure of the oligomer could be achieved in a short time. For cross-linking the precursor, the setups were heated in a furnace for 6 h at 370 °C (glass tube) or 430 °C (steel container). Using lower temperatures resulted in incomplete cross-linking. The deformation of the cross-linked precursor was measured by thermo-mechanical analysis (TMA 2000, Baehr, ground force: 1 N, pulsed force: 1 N, frequency: 0.1 Hz) in the temperature range of 25–300 °C in Ar with a heating rate of 5 °C/min.

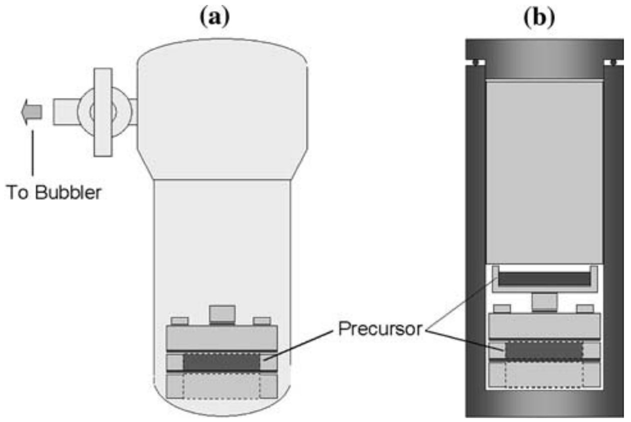

Fig. 1 Open glass tube (**a**) and sealed stainless steel container (**b**) used for cross-linking

After the cross-linking, the samples were demolded, and pyrolyzed subsequently at 1350 °C for 2 h in Ar (Ar 4.8, purity: >99.998 vol%, Messer). The heating rates for the first and following cycles were 1 °C/min and 5 °C/min, respectively. In order to avoid oxidation of the samples during pyrolysis as much as possible, the argon gas was pre-treated with a gas purification system (oxisorb®, Messer) [17]. The cycle of impregnation and pyrolysis was repeated up to 10 times.

The true density of the CMC (ρ_{CMC}) was calculated after each cycle by using the equation, $\rho_{CMC} = t_{carbon} \cdot \rho_{carbon} + t_{SiC} \cdot \rho_{SiC} + t_{Si–C–N} \cdot \rho_{Si–C–N}$ ($\rho_{carbon} = 1.81$ g/cm^3, $\rho_{SiC} = 3.22$ g/cm^3, $\rho_{Si–C–N} = 2.56$ g/cm^3) [18]. The volume fraction of the carbon fibers (t_{carbon}), the SiC filler (t_{SiC}), and the Si–C–N matrix ($t_{Si–C–N}$) was estimated by measuring the weight and true density of each component, respectively. The bulk density of the CMC with increasing the number of impregnation/pyrolysis cycles was estimated by dimensional measurement.

Thermo-gravimetric analysis (TGA, STA 501, Netzsch) of the CMC was performed in flowing Ar (100 mL/min) in the temperature range of 25–2100 °C with a heating rate of 3 °C/min.

The as-fabricated CMC was machined into bars (30 × 1.5 × 2 mm) and polished up to 1 µm finish. Subsequently, four point bending strength was measured (1476, Zwick GmbH, upper and lower span: 7 and 20 mm, respectively). A part of the testing samples were heated at 1350 °C for 24 h in Ar using an alumina tube furnace. Subsequently, the microstructure and phase evolution of the as-fabricated or the heated CMC were analyzed by optical microscopy (DM RM, Leica), scanning electron microscopy (SEM, Stereoscan 200, Oxford), energy dispersive spectroscopy (EDS, Phoenix, EDAX), and X-ray powder diffraction using CuK_α radiation (XRD, D 5000, Siemens), respectively. The four point bending strength was measured with a universal testing machine (Hydropuls® PSA, Schenck, upper span: 7 mm, lower span: 20 mm, five as-fabricated samples, three heated samples).

Results and discussion

Cross-linking

For a controlled cross-linking in the glass tube (Fig. 1a), the precursor had to be heated slowly. Due to bubble formation and foaming, the precursor became opaque when heated too fast. For fast heating, the total time to reach the cross-linking temperature was set as 160 min. In contrast, a dense and transparent polymer was obtained when a slow heating schedule was applied (total heating time up to 370 °C: 900 min). Bahloul et al. pointed out that there is a competition between cross-linking and evaporation. When heating is too fast, evaporation of low molecular weight oligomers occurs intensively before cross-linking can take place [19].

Since impregnation and pyrolysis must be repeated several times to obtain dense samples, slow cross-linking significantly increases the total processing time. Therefore, fast heating (160 min) was applied with suppressing the evaporation of oligomers by the application of a sealed container with an additional source of oligomer as described above and shown in Fig. 1b. By the application of the sealed stainless steel container, the total cross-linking time was expected to reduce to a quarter compared to using the conventional glass tube process, which would be in total 5 days after 10 PIP cycles.

Figure 2 shows the weight gain of the CMC cross-linked with the two different equipments as a function of the number of impregnation/pyrolysis cycle. Generally, the efficiency of process cycle decreases by the repetition, which is a consequence of the formation of closed pores [12]. The low weight gain after the first cycle was due to the high relative density of the SiC_{filler}/C_{fiber} compact and decomposition of surface SiO_2 layer formed on the SiC filler particles during the first pyrolysis step. The regarding phenomena will be discussed in the following paragraphs. The weight gain increased during the second pyrolysis step due to the increased free space in the compact caused by the swelling of the CMC during the first pyrolysis. The efficiency of PIP decreased at the third cycle.

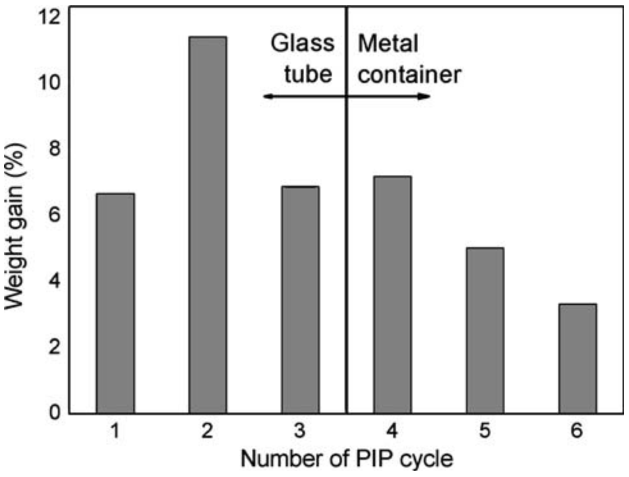

Fig. 2 Weight gain of the CMC after the application of different cross-linking equipments using fast heating rate and subsequent pyrolysis

The metal container increased the efficiency of the PIP cycles even when the sample was pre-densified three times in the glass tube. This is due to the fact that the oligomers could escape freely through the bubbler in the glass tube, while such evaporation was suppressed in the closed metal container. Kroke et al. [20] reported that the most important prerequisite to raise ceramic yields during pyrolysis is to prevent evolution of volatile Si-containing species.

Beside the mass loss, another important problem during the cross-linking of the polymer is the formation of bubbles. Bubbles were formed by the evaporation of oligomers and were transformed to defects during pyrolysis. In order to prevent the formation of bubbles, slow heating must be applied during cross-linking when using glass tube. In contrast, the high pressure inside the metal container efficiently suppressed the evaporation of oligomers and so did the bubble formation even during the fast heating.

Densification, microstructure, and mechanical property

The chemical composition of the Si–C–N precursor after the cross-linking and pyrolysis at 1350 °C for 2 h in Ar was measured to be $SiC_{0.68}N_{0.91}$ [20].

Figure 3 shows the relative density of the CMC samples as a function of the number of impregnation/pyrolysis cycles. The relative density of the stacked woven fabrics was estimated to be 39%. After the infiltration of the SiC slurry, the relative density of the C_{fiber}/SiC_{filler} compact increased to 71%. The value decreased due to a swelling during the first pyrolysis cycle, which was a consequence of the gas formation during pyrolysis and the softening of the cross-linked precursor. TMA measured the dimension

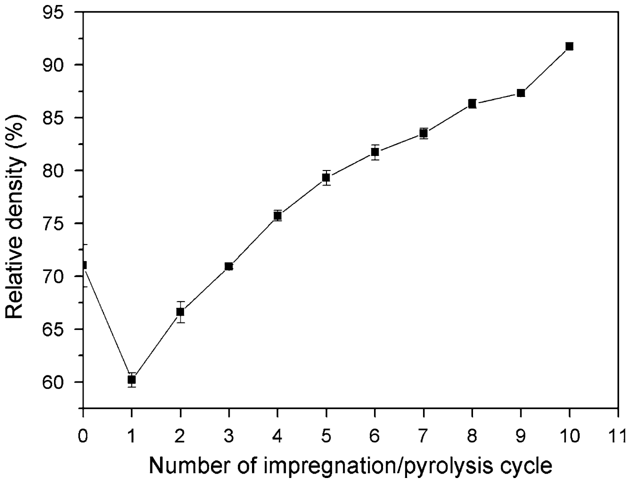

Fig. 3 Relative density of the CMC vs. number of impregnation/pyrolysis cycles using the stainless steel container for cross-linking

of the specimen with changing temperature and applied force. During the measurement, the dimension of the specimen increased linearly due to thermal expansion below 150 °C. The viscosity of the precursor decreased above 175 °C by softening, thus the specimen could be more easily deformed by the repeatedly applied force [21]. As a result, the amplitute of the TMA data increased above 175 °C (Fig. 4). The precursor compact shrank above 200 °C because it could not sustain the pressure for TMA measurement.

The relative density of the CMC was 92% (2.14 g/cm^3) after the 10th PIP cycle [21, 22]. The swelling of the CMC did not occur after the second PIP cycle due to the formation of a rigid Si–C–N ceramic network. The swelling increased the free space in the samples. As a result, the amount of the impregnated liquid precursor increased at the second processing cycle. Importantly, the formation of macropores at the free space between the bundles or woven fabrics was clearly suppressed by using the modified SiC slurry infiltration process (Fig. 5a, b) [14].

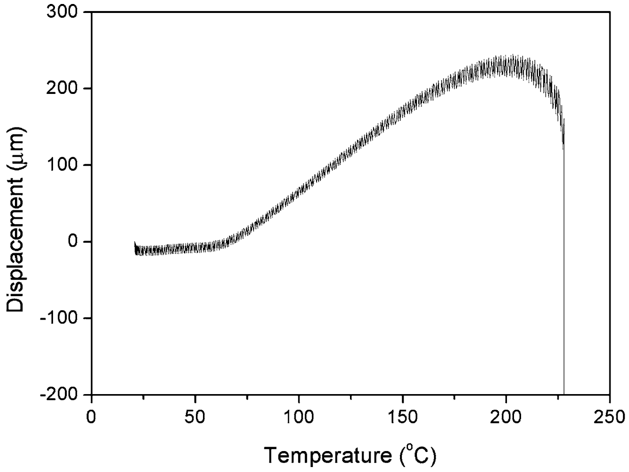

Fig. 4 TMA data of the cross-linked precursor (Ar, 5 K/min). Thermal expansion of the precursor became distinct above 60 °C. The amplitude of vibrations increased above 175 °C due to the softening of the precursor. The sample shrank above 200 °C due to the softening. The precursor compact was broken at 230 °C

Cracks were observed in the as-fabricated CMC. A part of the cracks formed a regular array and existed even after repeated impregnation and pyrolysis cycles (Fig. 5a). The coefficient of thermal expansion (CTE) of the carbon fiber is largely different from those of the other two components used for the CMC (SiC: 4.5–4.9 × 10^{-6}/K, Si–C–N: 3.2 × 10^{-6}/K, carbon: ~0/K) [23]. The difference caused cracking during the cooling of the CMC.

Fine microcracks were observed in areas in between the layers of woven fabrics (Fig. 5b). They were presumably originated from the shrinkage of the infiltrated SiC slurry during drying and/or from the swelling of the CMC during the first pyrolysis. The microcracks could not be removed completely by the repeated PIP cycles.

The average value of the maximum strength was 286 MPa (standard deviation: ±32 MPa). The strength of C_{fiber}/Si–C–N_{matrix} CMC made by PIP technique has been frequently reported to be lower than 200 MPa (125 MPa, 150–200 MPa) due to the presence of cracks [24, 25]. The relatively high strength of the CMC in the present investigation was partly attributed to the absence of the macro-interyarn pores by using the modified slurry infiltration technique.

The fiber-reinforced CMC showed excellent damage tolerance. Due to their pyrocarbon coating, the carbon fiber provided a weak bonding with the matrix [26]. Cracks propagated predominantly along this coating (Fig. 5c), and fiber pull-out (>400 μm) was observed at the fracture surface (Fig. 5d). The entire bar samples were bent during the strength measurement, and did not show brittle fracture. The fibers bent and bridged the fractured parts (Fig. 5e).

High temperature stability

Although the deterioration of the CMC was not expected at 1350 °C in Ar due to the thermal stability of the constituents, the CMC retained only 73% of the original strength after a heating for 24 h (286 vs. 209 MPa). Accordingly, the possible reasons for the deterioration were analyzed.

Figure 6 shows TGA data of the Si–C–N ceramics and the C_{fiber}/SiC_{filler}/Si–C–N_{matrix} CMC up to 2100 °C in Ar. The amorphous Si–C–N ceramics have been reported to crystallize above 1300 °C into Si_3N_4, SiC, and free carbon [27]. Consequently, the mass loss of Si–C–N (curve a) above 1450 °C has been attributed to the reaction of Si_3N_4 with free carbon and the degassing of nitrogen [28]. The reaction became less intensive above 1700 °C due to the consumption of the reactants. At 2100 °C, the total weight loss of the Si–C–N was 26.5 wt%.

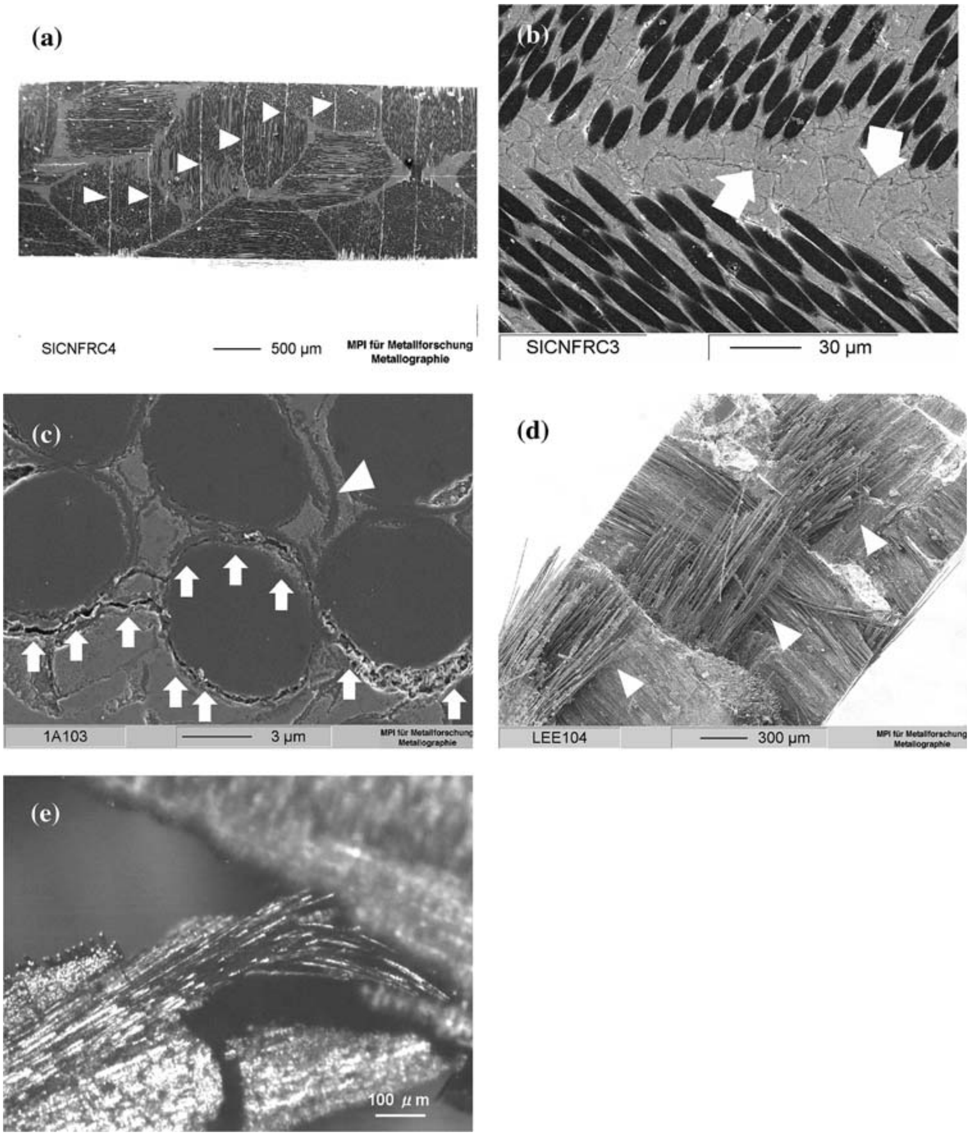

Fig. 5 Cracks, flaws, and fiber pull-out in the CMC. **a** arrays of cracks observed at the polished surface (▷) by the difference of CTE between the fiber and the matrix, **b** microcracks in the matrix located between fiber bundles (⇨), **c** cracks propagate through the pyrocarbon coatings (⇨: crack propagation, ▷: detached coating), **d** fiber pull-out (▷: pulled-out fibers at different layers) and **e** fiber bending and Bridging

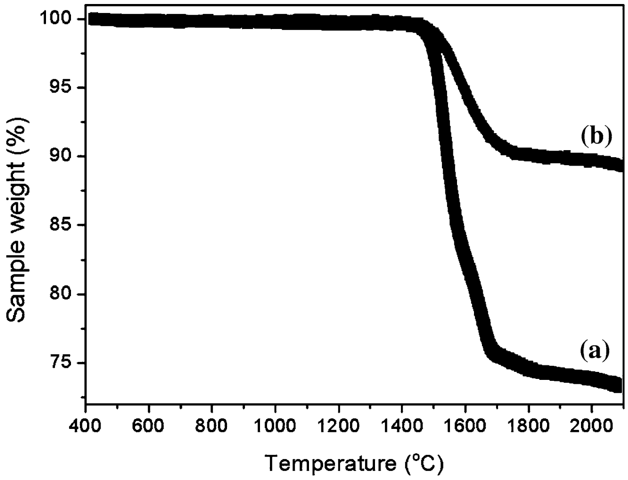

Fig. 6 High temperature TGA of, (a) Si–C–N bulk ceramics and (b) $C_{fiber}/SiC_{filler}/Si–C–N_{matrix}$ CMC

The total weight loss of the CMC (Fig. 6b) was 10.7%. Both SiC and carbon are thermally stable up to 2100 °C [29]. Because the content of the Si–C–N within the CMC was 33.2 wt%, the mass loss of the Si–C–N matrix in the CMC was estimated to be 32.4 wt%. This value is higher than that of the pure Si–C–N.

SiC has been used as a filler for PIP process, but the detrimental effect of surface SiO_2 on the filler has been rarely considered. The SiO_2 surface layer of the SiC filler induced weight loss above 1500 °C in Ar by the reaction with SiC according to [30];

$$2SiO_{2(s)} + SiC_{(s)} \rightarrow 3SiO_{(g)} + CO_{(g)}, \qquad (1)$$

and/or with the carbon of the surrounding Si–C–N matrix and carbon fiber above 1200 °C; [31]

$$SiO_{2(s)} + C_{(s)} \rightarrow SiO_{(g)} + CO_{(g)}, \qquad (2)$$

$$SiO_{2(s)} + 3C_{(s)} \rightarrow SiC_{(s)} + 2CO_{(g)}. \quad (3)$$

The oxygen content of the SiC powder used in the present investigation was 0.9 wt% [14]. The value corresponds to 1.7 wt% of SiO_2 and this oxide reacts and additionally consumes 1.1 wt% of SiC by reaction (1), 0.3 wt% of carbon by reaction (2) and 1.0 wt% of carbon by reaction (3). The mass loss of reaction (3) was partly compensated by the formation of SiC (1.1 wt%). Therefore, the mass loss by reaction (1), (2), and (3) is calculated to be 2.8, 2.0, and 1.6 wt%, respectively, when containing 0.9 wt% of oxygen in the CMC. Because the CMC contained 38.2 wt% of the SiC filler, the total oxygen content of the CMC and consequent mass loss by reactions (1), (2), and (3) are estimated to be 0.3 wt% and 1.06, 0.76, 0.58 wt%, respectively.

After the heating of the CMC at 1350 °C for 24 h in Ar, a coating which has a bright contrast was observed on the surface of the samples by SEM (Fig. 7a). Figure 8 shows the XRD patterns of the CMC before and after the heating. The main peak of cristobalite (SiO_2), which was not overlapped by SiC peaks, was detected in the heated sample. EDS analysis confirmed that the coating was mainly composed of SiO_2 (Fig. 7b). Only minute burn-out of carbon fibers was observed beneath the white coating (Fig. 8a), indicating that the SiO_2 was not formed by the passive oxidation of SiC and the Si–C–N matrix; otherwise the carbon fibers should be heavily damaged.

The above results indicate that SiO_2 formed on the SiC filler partly remained after the fabrication and induced thermal decomposition by reaction (2) and (3) during the heating of the CMC at high temperatures and/or prolonged time. The oxygen partial pressure within the CMC is believed to be low by the reaction with the free carbon contained in the Si–C–N matrix and carbon fibers. Accordingly, residual SiO_2 in the CMC could be presumably easily decomposed. SiO gas thus formed was migrated to the surface through the open pores and reacted with oxygen which was supplied from the atmosphere according to [31];

$$2SiO_{(g)} + O_{2(g)} \rightarrow 2SiO_{2(s)}. \quad (4)$$

The slight burn-out of the carbon fibers at the surface areas of the specimens (depth of the area: $\leq$20 μm,

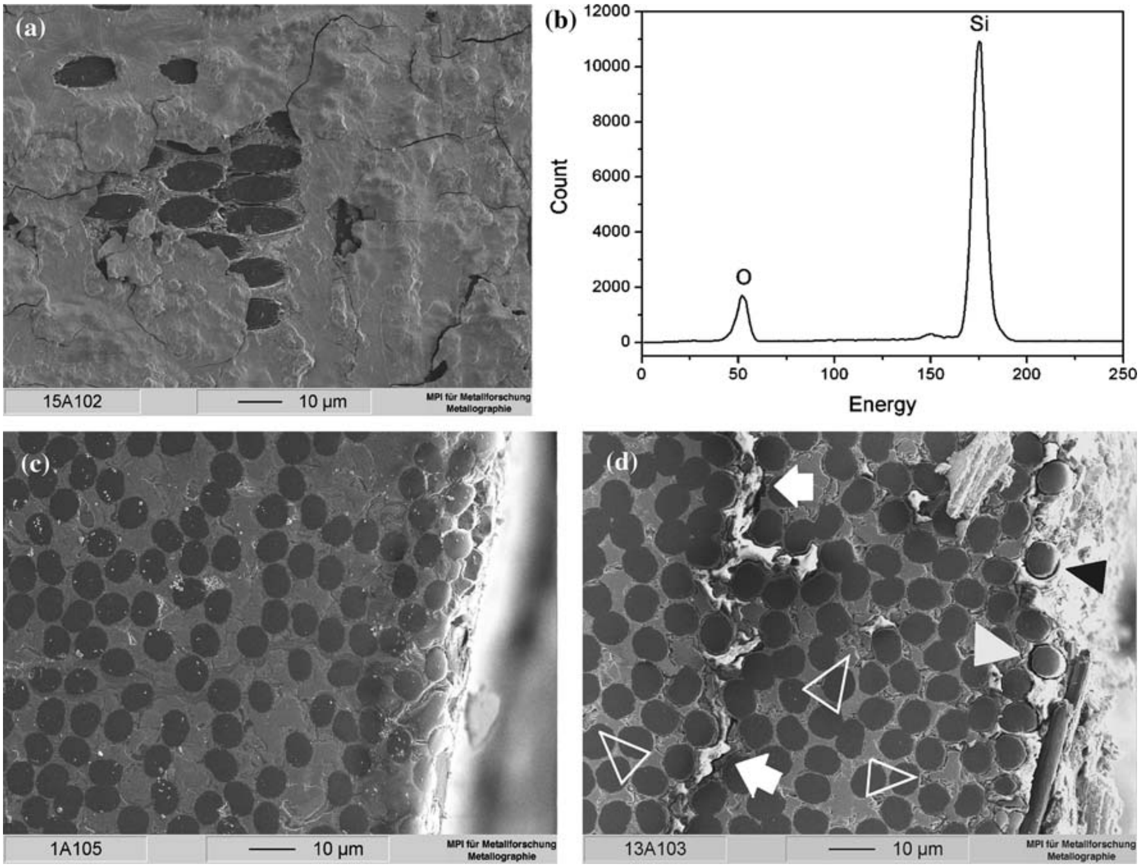

Fig. 7 Morphology of the CMC. **a** Formation of a white coating at the surface of the CMC. **b** EDS data of the white coating. **c** Cross-sectional morphology of surface-near area before the heating. Deterioration of the fibers or the matrix is not observed, and **d** after the heating. (▶: fiber-matrix debonding by a slight burn-out of the fiber, ▷: damaged matrix, ⇨: crack)

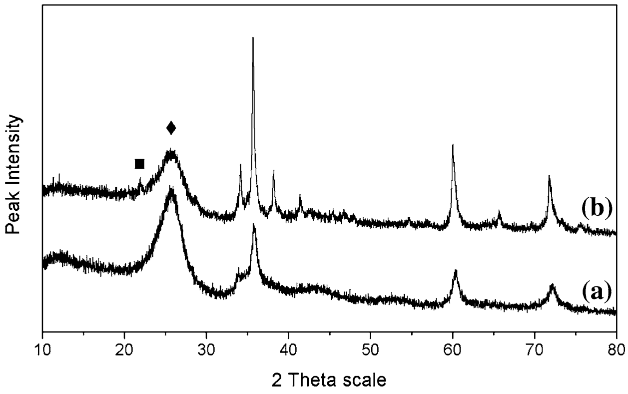

Fig. 8 XRD data of the CMC (a) before, and (b) after the heating at 1350°C for 24 h in Ar. (■: cristobalite, ◆: graphite, and others: SiC)

Fig. 7d) indicated the presence of oxygen in Ar. The weight loss of the CMC after the heating was 2.8 wt%.

In contrast to the dense matrix of the as-fabricated CMC (Fig. 7c), microcracks were formed in the matrix of the heated specimen, (Fig. 7d). The decomposition of SiO_2 by reaction (2) and (3) was believed to induce the damage of the matrix, which partly attributes to the loss of strength during the heating of the $C_{fiber}/SiC_{filler}/Si–C–N_{matrix}$ CMC.

Figure 9a and b show fractured surfaces of the CMC samples before and after the heating, respectively. Clear detachment of the fibers was observed in the fractured surface of the as-fabricated CMC. In contrast, the fibers were adhered by a reaction product after the heating (Fig. 9b). The pulled-out fibers within the heated CMC were also coated with the reaction product (Fig. 9c). The formation of whiskers was also observed in the heated specimens. EDS data informed that the product formed at the surface of the carbon fiber and the whiskers was SiC (Fig. 9d).

Once SiO gas is formed by reaction (1) and (2), it reacts with carbon in the matrix and the fiber according to [32];

$$SiO_{(g)} + 2C_{(s)} \rightarrow SiC_{(s)} + CO_{(g)}. \quad (5)$$

The damage of the fibers is believed to be another main reason for the deterioration of the CMC after the heating. The attachment of SiC by reaction (5) and consequent damage of the fiber occurred even inside the specimens, which was evident from the pulled-out fibers (Fig. 9c).

The above discussion indicates that the main reasons for the deterioration of the heated CMC were the weakening of the matrix and the deterioration of carbon fibers. In both

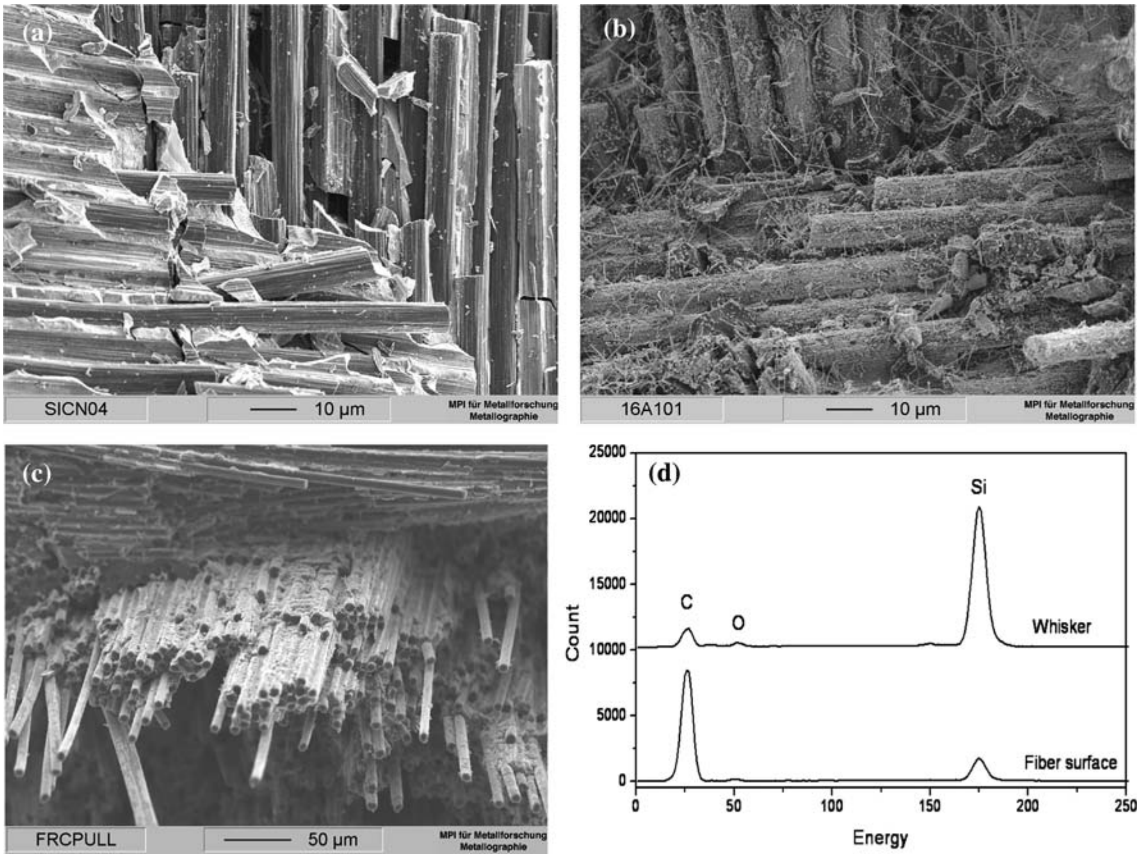

Fig. 9 Morphology of fractured surface of the CMC before and after the heating at 1350 °C for 24 h in Ar. **a** before the heating, **b** after the heating, **c** over view of fiber pull-out after the heating, and **d** EDS data of the damaged fiber surface and the whisker

cases, SiO_2 layer at the surface of the filler particles played an important role.

Summary and conclusions

The cross-linking time for the production of the CMC was reduced and flaw formation was suppressed by the application of a sealed metal container. The suppression of the vaporization of oligomers during cross-linking was important to improve the efficiency of the PIP process. Swelling of the CMC occurred during the first pyrolysis due to the softening of the cross-linked precursor. Room temperature bending strength of the CMC was 286 MPa. The CMC retained 77% of the original strength after a heating at 1350 °C for 24 h in Ar. The deterioration of the CMC after the heating was attributed to the weakening of the SiC_{filler}/Si–C–N matrix and damage of the carbon fibers by the decomposition of surface SiO_2 layer formed on SiC filler.

References

1. Flegel HA (2001) In: Heinrich JG, Aldinger F (eds) Ceramic materials and components for engines. Wiley, Weinheim, p 3
2. Christin F (2001) In: Krenkel W, Naslain R, Schneider H (eds) High temperature ceramic matrix composites. Wiley, Weinheim, p 732
3. El-Hija HA, Krenkel W (2001) In: Krenkel W, Naslain R, Schneider H (eds) High temperature ceramic matrix composites. Wiley, Weinheim, p 846
4. Luthra KL, Corman GS (2001) In: Krenkel W, Naslain R, Schneider H (eds) High temperature ceramic matrix composites. Wiley, Weinheim, p 744
5. Baldus P, Jansen M, Sporn D (1999) Science 285(30):699
6. Sugimoto M, Morita Y, Seguchi T, Okamura K (1999) In: Niihara K (ed) Key engineering materials, vol 164–165. Trans Tech Publication, Zuerich, p 11
7. Riedel R, Kienzle A, Ruwisch W, Bill J, Aldinger F (1996) Nature 382(6594):796
8. Choong Kwet Yive NS, Corriu RJP, Leclercq D, Mutin PH, Vioux A (1992) Chem Mater 4(1):141
9. Li YL, Kroke E, Riedel R, Fasel C, Gervais C, Babonneau F (2001) Appl Organomet Chem 15(10):820
10. Tanaka T, Tamari N, Kondoh I, Iwasa M (1995) J Ceram Soc Jpn 103(1):1
11. Greil P (1995) J Am Ceram Soc 78(4):835
12. Nakano K, Kamiya A, Nishino Y, Imura T, Chou TW (1995) J Am Ceram Soc 78(10):2811
13. Tanaka T, Tamari N, Kondo I, Iwasa M (1998) Ceram Int 24(5):365
14. Lee SH, Weinmann W, Aldinger F (2007) J Am Ceram Soc 90(8):2657
15. Technical reference from the producer. http://www.starfiresystems.com/download.cfm/SMP_10_Storage_and_Handling.pdf?AssetID=162
16. Technical reference from the producer. http://www.kioncorp.com/bulletins/general.html
17. Lee SH, Weinmann M, Aldinger F (2005) J Am Ceram Soc 88(11):3024
18. Technical reference from the producer. http://www.torayca.com/techref/index.html
19. Bahloul D, Pereira M, Goursat P, Choong Kwet Yive NS, Corriu RJP (1993) J Am Ceram Soc 76(5):1156
20. Kroke E, Li YL, Konetschny C, Lecomte E, Fasel C, Riedel R (2000) Mater Sci Eng 26(4–6):97
21. Seitz J, Bill J (1996) J Mater Sci Lett 15(5):391
22. Zheng G, Sano H, Uchiyama Y, Kobayashi K, Suzuki K, Cheng H (1998) J Ceram Soc Jpn 106(12):1155
23. Nechanicky MA, Chew KW, Sellinger A, Laine RM (2000) J Eur Ceram Soc 20(4):441
24. Ziegler G, Richter I, Suttor D (1999) Compos part A 30(4):411
25. Rothe B, Suttor D, Ziegler G (1999) In: Niihara K (ed) Key engineering materials, vol 164–165. Trans Tech Publication, Zuerich, p 103
26. Helmer T, Peterlik H, Kromp K (1995) J Am Ceram Soc 78(1):133
27. Iwamoto Y, Voelger W, Kroke E, Riedel R (2001) J Am Ceram Soc 84(10):2170
28. Peng J (2002) Thermochemistry and constitution of precursor-derived Si–(B–)C–N ceramics, PhD Thesis, University of Stuttgart, Stuttgart
29. Rak Z (2001) J Am Ceram Soc 84(10):2235
30. Bibbo GS, Benson PM, Pantano CG (1991) J Mater Sci 26(18):5075. doi:10.1007/BF00549894
31. Colombo P, Modesti M (1999) J Sol–Gel Sci Techol 14(1):103
32. Wang L, Wada H, Allard LF (1992) J Mater Res 7(1):148